International Journal of Marine Energy 17 (2017) 136–146

Contents lists available at ScienceDirect

International Journal of Marine Energy

journal homepage: www.elsevier.com/locate/ijome

The influence of blade roughness on the performance of a vertical axis tidal turbine

Luis Priegue, Thorsten Stoesser *

Cardiff School of Engineering, Trevithick Building, 14-17 The Parade, Cardiff, United Kingdom

ARTICLE INFO

Article history:
Received 12 January 2016
Revised 10 October 2016
Accepted 11 January 2017
Available online 13 January 2017

Keywords:
Blade roughness
Vertical axis tidal turbine
Cross-flow turbine
Physical experiments

ABSTRACT

This paper reports the findings of an experimental study investigating the influence of blade roughness on the performance of a vertical axis tidal turbine. Due to their design, vertical axis turbines undergo periods of stall, i.e. flow separation from the blade, during each revolution. It is hypothesised that roughening turbine blades delays flow separation (in analogy to flows over rough bluff bodies) and hence diminishes turbine stall which in turn should result in an increase in turbine performance. Laboratory experiments were undertaken in Cardiff University's hydraulics laboratory, testing vertical axis turbines with rotors comprising smooth and rough blades. Three different blade surface roughnesses were tested, with the results showing a significant reduction in performance when the turbine is operating at high chord Reynolds numbers and with rough blades. In addition, the combined effect of blade roughness and rotor solidity as well as blade roughness and number-of-blades on the performance of vertical axis turbines are analysed. It is shown that solidity and number-of-blades appear to be similarly influential than blade roughness.

1. Introduction

With fossil fuel resources slowly dwindling there remains the pressing need of exploiting other resources of energy. The fact that tidal stream energy is renewable and predictable makes it a promising alternative resource. Tidal stream energy is extracted by tidal turbines, the design of which is similar to wind turbines and nowadays most tidal turbine developers are employing the horizontal axis tidal turbine (HATT) concept, mainly due to its high efficiency (above 35%) [1] and its fairly straight-forward operating principle [2,3]. Vertical axis tidal turbines (VATT) are an attractive alternative to HATTs, mainly because of their omni-directionality, which is advantageous in tidal streams where the direction of flow changes approximately every six hours. Additionally, a VATT design may allow for placing the power take-off above the water surface, which simplifies turbine maintenance thereby reducing costs [4]. Despite their advantages, vertical axis or cross-flow hydrokinetic turbines have not received as much attention as their more attractive horizontal axis counterpart, probably on account of their inferior hydrodynamics and complex fluid–structure interaction. Nonetheless, they have become the subject of increased interest in recent decades due to their suitability to operate in shallow coastal waters, rivers or canals, because of their square (or rectangular) cross-sectional area, which makes a more efficient use of the available water depth [5,6]. These advantages and reasonably high efficiency values (25–35%) have triggered several studies researching the performance of VATTs, e.g. [7,8]. However, certain drawbacks persist: most importantly the constantly changing angle of attack

* Corresponding author.
E-mail address: stoesser@cf.ac.uk (T. Stoesser).

http://dx.doi.org/10.1016/j.ijome.2017.01.009
2214-1669/

on the blades which means that fixed-pitch blades are subjected to static stall and uneven loading and in addition the continued difficulty of making the turbine self-start without sacrificing performance, e.g. a five-bladed rotor will most certainly self-start but is significantly less efficient than a two-bladed rotor which most likely won't self-start. A design challenge is that VATTs offer a large number of rotor parameters such as blade shape, pitch and angle of twist, rotor solidity, shaft diameter, number-of-blades all of which are known to influence rotor performance [9] and even blade roughness can play a significant role e.g. [10,11] and as will be shown in this paper. Thus, the emergence of the perfect VATT appears elusive so far. Due to the complex intertwine of above mentioned turbine parameters the few experimental studies reported in the literature cannot give a full explanation as to why certain turbine design parameters work better than others, which is complicated by the fact that different experiments were conducted under different conditions (e.g. different blade Reynolds numbers, channel blockage, etc). There are several numerical studies that have shed some light onto the flow-turbine interaction, e.g. [12–16], but these focused mostly on complementing existing laboratory studies and have not investigated in detail the impact of various turbine parameters on VATT performance.

VATT design might benefit from many years of research into the optimization of Darrieus-type vertical axis wind turbines, e.g. [17–19], however there are significant differences between wind and water in terms of approach flow speed and fluid properties. Hence, and similar to horizontal axis tidal turbine research, knowledge transfer from wind to water is not straightforward. For instance, most Darrieus-type wind turbines feature symmetric NACA aerofoils, achieving fairly good performance [20–22], but it has been shown that asymmetric or cambered hydrofoils can outperform the results from symmetric hydrofoils for some VATT designs [23,24]. The number of blades and rotor solidity are two of the main design parameters being considered for VATTs and these have been tested to some extent, although the range of optimum values remains wide [25,26]. An attempt to overcome self-starting problems and uneven loading is the Gorlov turbine design [27], which employs helical turbine blades and therefore increases the area swept by the rotor along its circumference. The flip side of this innovation is that power output is decreasing with increasing angle of twist [26]. One important aspect in the design of Darrieus-type turbines is the choice of blade shape and its lift-to-drag ratio, [28,29]. Generally, for any lift-driven turbine, the greater this ratio, the better the performance of the turbine. The influence of surface roughness on the lift-to-drag ratio of an airfoil was analysed by some researchers [30,31] who concluded that smooth-surface blades cause greater lift and less drag compared with rough-surface blades. Nevertheless, the results must be used carefully because these studies did not consider the influence of rotation and/or flow curvature, respectively and hence did not investigate the airfoil blade's behavior during stall.

Walker et al. [11] investigated the effects of blade roughness on the performance of a horizontal axis tidal turbine (HATT). They conclude that rough blades diminish turbine performance by 19%, however HATTs operate at much higher tip-speed ratios than VATTs and dynamic stall is not a critical design issue. The effect of blade roughness on vertical axis wind turbine performance was analysed in [10]. In this work, rough-bladed turbines performed better than smooth-bladed turbines at fairly low chord Reynolds numbers but at higher chord Reynolds number flows smooth-bladed turbines outperformed rough-bladed turbines. They pointed out the competition between skin friction and form drag in analogy to the flow around a rough bluff body, e.g. [32], i.e. in the critical flow regime increased surface roughness delays flow separation and thus reduces form drag (of the blade) which increases turbine performance. Once a critical Reynolds number is surpassed the increase of friction drag cannot be compensated for by a reduction in form drag. For airfoils Lissaman [33] suggests this critical chord Reynolds number to be around 10^5 below which rough-bladed airfoils exhibit a greater lift-to-drag-ratio than smooth-bladed airfoils.

Several studies, e.g. [13,34,35], have revealed that dynamic-stall-generated vortices result in a sudden and significant increase in drag which in turn results in a sudden drop of the power coefficient. The motivation of this study is based on the hypothesis that blade roughness could delay flow separation and hence could reduce the shed stall-vortex, e.g. in the way sketched in Fig. 1. This paper reports on a series of laboratory tests that were carried out in the hydraulics laboratory at Cardiff University with the goal to quantify the performance of a vertical axis turbine comprising blades made of three different blade materials, each with a different surface roughness. The results will clarify whether blade roughness enhances (or diminishes) VATT performance.

2. Experimental setup

The tests were carried out in the laboratory flume in the School of Engineering at Cardiff University. The flume is 17 m long and 1.2 m wide and the flow is driven by an axial flow impeller, which enables a maximum flow speed of 1.3 m/s at 0.5 m water depth. Fig. 2(a) sketches the turbine inside the laboratory flume. The rotor was held in place by two roller bearings, one mounted on the bottom of the flume and the second on the cross-beam above the flume. DVE Technology's (http://www.dvetech.com/) 200 W permanent magnet generator (PMG) was attached to the end of the shaft and above the water surface.

The electrical circuit, which is depicted on the right hand side of Fig. 2(b), consisted of a rectifier (AC/DC), changing the current from AC to DC, a load bank comprising two variable resistors in series (R_1 and R_2) rated at 20 Ω each and a Fluke 123/S oscilloscope (A) with which the electrical current I_A was measured during the experiment. Additionally, an optical tachometer was used to determine the rotational speed (ω) of the rotor. With the measured quantities the electrical power (P_e) of the generator is computed as:

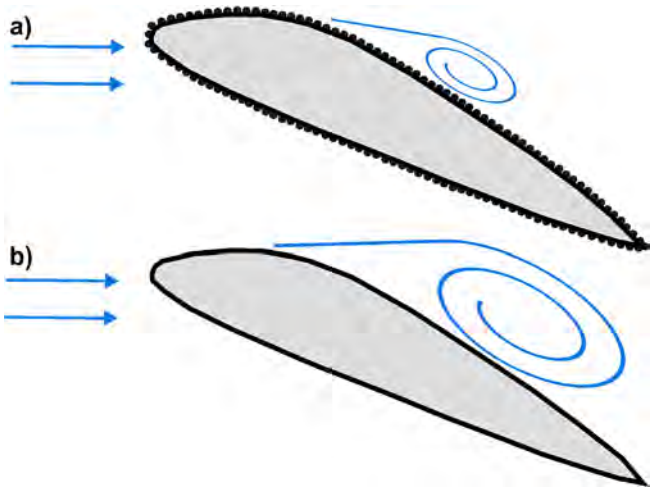

Fig. 1. Possible flow separation from vertical axis turbine blades at high angle of attack: (a) rough blade; (b) smooth blade.

$$P_e = \omega T_e \tag{1}$$

where T_e is the electrical torque obtained from:

$$T_e = K_G I_A \tag{2}$$

where K_G is a generator-specific constant relating voltage to rotational speed and it was provided by the generator manufacturer. The available experimental data of this study confirms the magnitude of K_G, which is shown in Fig. 2(c). The oscilloscope has a sampling rate of 25 Ms/s at a bandwidth of 20 Hz [36] and the sampling rate of the optical tachometer is 4 reads per revolution of the turbine (using 4 reflective marks on the generator) which spins at approximately 120 rpm.

Turbine characteristics curves, i.e. turbine efficiency as a function of its rotational speed were obtained by varying the electrical load on the generator using two resistors, which allowed controlling the rotational speed, ω, of the turbine. The turbine was operated between "close-to-free-wheeling" and turbine-stall by varying $R1 + R2$ between 40 Ω (close-to-free-wheeling) and ≈ 5Ω (which is approximately where the turbine stalled). For every increment of the resistance, average rotational speed, ω, and electrical current were measured over a 60s interval. The turbine efficiency, also referred to as coefficient of power (C_p) was then calculated for each ω as:

$$C_p = \frac{P_e}{\frac{1}{2}\rho A U_0^3} \tag{3}$$

where ρ is the density of the water, A is the projected area of the turbine and U_0 is the average approach flow velocity. The turbine efficiency is usually plotted as a function of tip-speed-ratio, λ, which is defined as:

$$\lambda = \frac{\omega D}{2U_0} \tag{4}$$

where D is the diameter of the turbine. λ relates the velocity of the blade to the approach velocity. Another important velocity in the operation of a vertical axis turbine is the relative speed, w, which is the vector sum of the rotational speed, $v = \omega D/2$, and approach flow U_0, as sketched in Fig. 3(a). w varies during one revolution of a vertical axis turbine, i.e. angles of rotation between $\theta = 0$ and $\theta = 360$ and w is a function of λ as:

$$w = v\sqrt{2\lambda\cos\theta + \lambda^2 + 1} \tag{5}$$

During operation of the turbine the angle of attack α changes constantly, and so does the lift-to-drag ratio. At large α the flow separates from the airfoil, known as dynamic stall, which leads to a sudden large increase in the drag force, d, and to zero or even negative lift force (l). Fig. 3(b) plots α as a function of angle of rotation θ for three different values of λ. The dashed line signifies high angles of attack at which stall is expected to occur and in particular at low λ stall occurs over substantial parts of the rotation.

The power curves do not explicitly quantify electrical losses. DVE Tech, the generator manufacturer, provide a value of 87% for generator efficiency and the rectifier losses are of the order of 3% (value provided by the manufacturer). The effect of flow blockage and frictional effects (e.g. friction in the bearings) on the turbine efficiency were not quantified explicitly in this study; they are the same for all turbines tested.

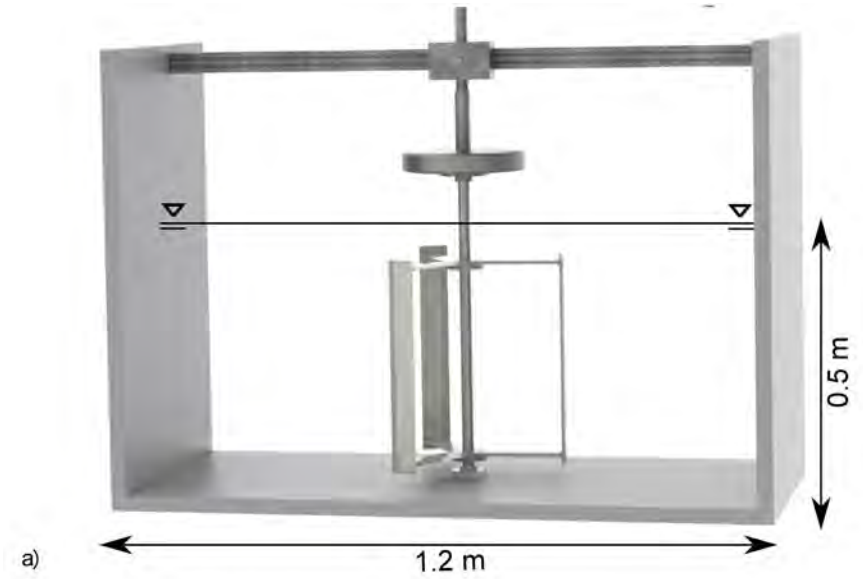

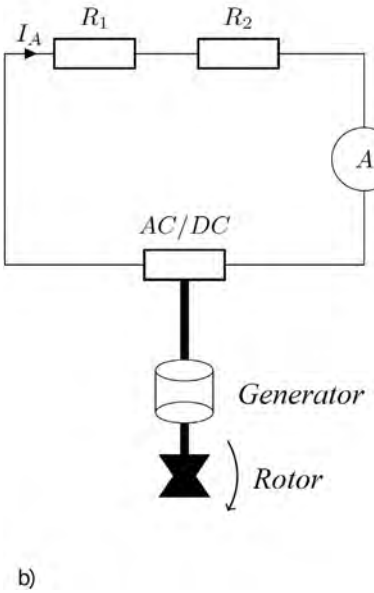

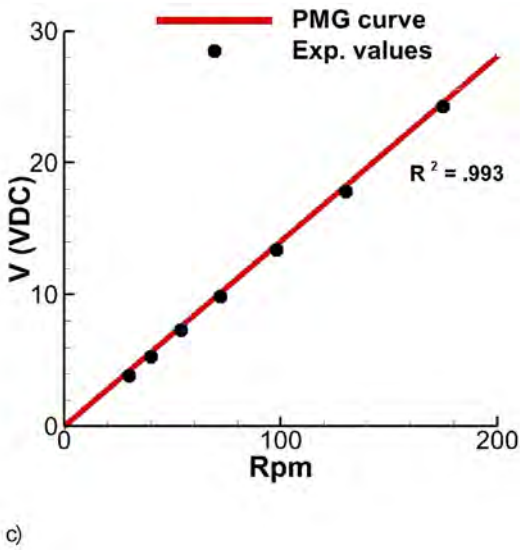

Fig. 2. Sketch of the setup of the laboratory experiment (a), the electrical circuit (b) and experimentally validated generator performance curve (c).

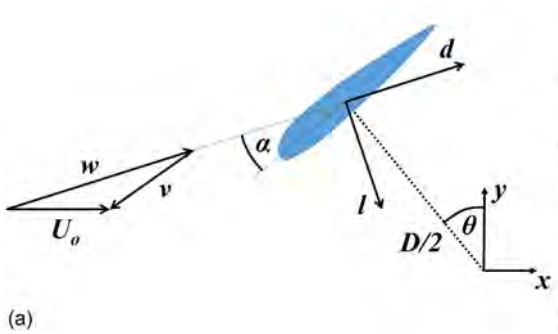

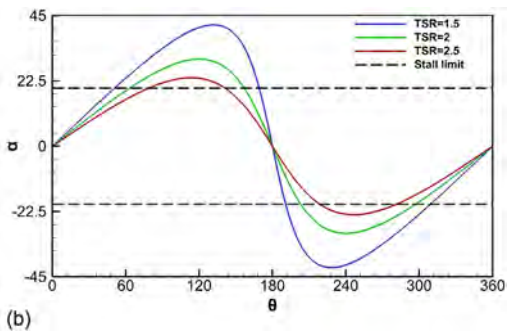

Fig. 3. Sketch of the main velocities and acting forces in a rotating system (a) and angle of attack α as a function of rotated angle θ at various tip speed ratios λ (b).

In this study, blades were manufactured from two different materials, polyethylen plastic (Material A) and polyamide thermoplastic (Material C). The blades of Material A were machined using a CNC machine with a 16 microinches surface finish. The blades of Material C were manufactured by a rapid prototyping procedure known as laser sintering which resulted in a rather rough blade surface. After testing the blades of Material C, they were sanded and painted in order to reduce their surface roughness which yielded an intermediate roughness and this material is referred to as Material B. The blade roughness was measured with a surface profiler and measurements were taken in the centerline along the chord. The instrument (Talysurf Series 2 – Taylor Hobson) consists of a contact-less gauge with namometric precision. The measurement data were analysed by the instrument's accompanying software to obtain the roughness statistics of each surface. An example of the blade surface profile of Material A and the software output in terms of statistical properties of the profile is presented in Fig. 4. The outputs of the roughness measurements and statistical properties of the three blades are summarized in Table 1.

In order to characterize the blades' hydrodynamic performance it is necessary to convert measured absolute roughness heights of the blade into relative (or sandpaper) roughness k_s, with the goal of classifying the roughness hydrodynamically following Nikuradse [37]. As Bons acknowledges [38], conversion from absolute roughness data to sandpaper roughness is not a trivial task. Bons [38] provides an excellent literature review of how absolute roughness is converted into k_s and there are many different conversion formulae (see Table 3 for references). For the three materials used in this study k_s values are provided in Table 2. They are obtained as an average of the 17 proposed conversions that are given in Table 3.

A hydrodynamic appreciation of blade roughness is obtained from the roughness Reynolds number (Re_*), which is calculated as:

$$Re_* = \frac{k_s u_*}{\nu} \tag{6}$$

where the friction velocity, u_* is estimated conservatively to be 10% of the relative velocity w, which is computed from Eq. 5 for the onset of stall, i.e. $\theta = 60^o$, see Fig. 3(b) and for $\lambda = 2.0$ which, on average, corresponds to peak power extraction. In this study, three different approach flow speeds were considered, i.e. $U_0 = 0.72,\ 0.98,\ 1.15$ m/s and, therefore, the blades of the different materials were subjected to a range of roughness Reynolds numbers. Minimum and maximum values of Re_* for each material and for each of the three approach flow velocities are provided in Table 2. The blades made of Material A are hydrodynamically smooth (i.e. $Re_* < 3$), and the ones made from Materials B and C are considered to be in the transitional range (i.e. $3 < Re_* < 100$). Blades made of Material C however are appreciably rougher than blades made of Materials A and B.

The turbine rotor was 0.28 m in height and had a radius of 0.2 m, which yielded an aspect ratio (height divided by diameter) of 0.7. Two 8 mm thick discs connected the blades to the shaft. The blades were shaped according to the Eppler 715 airfoil (Fig. 5), expecting that its asymmetric shape could provide a high lift-to-drag ratio. The set of experiments involved tests with three different chord lengths, i.e. c = 8, 10 and 12 cm and three approach flow speeds $U_0 = 0.72,\ 0.98,\ 1.15$ m/s

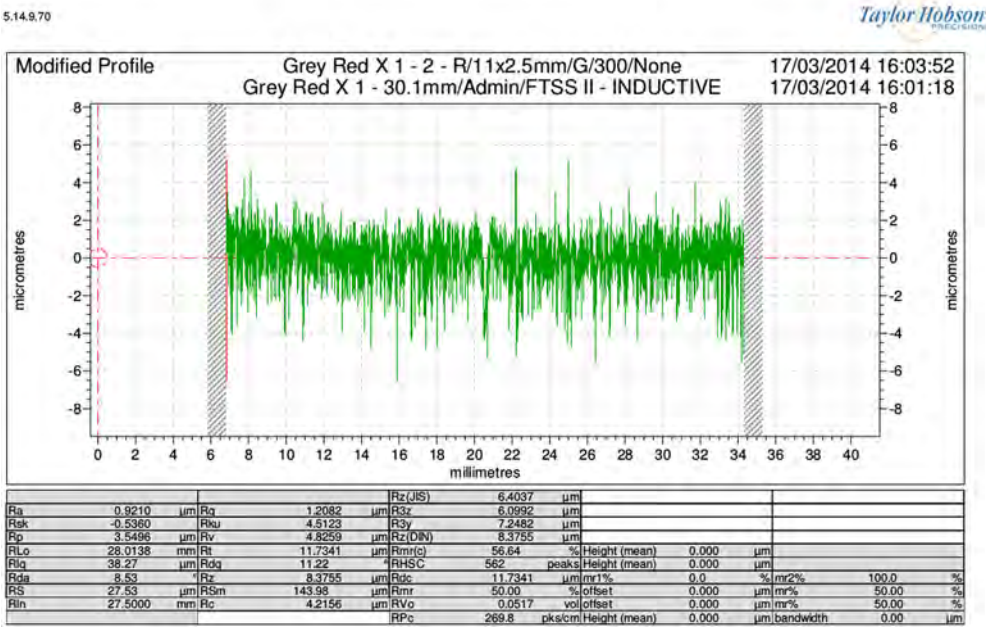

Fig. 4. Software output from Taylor Hobson's Talysurf 2. Spatial distribution of the blade surface elevations. Also provided as an output are the statistical data of the measurement, including the quantities listed in Table 1.

Table 1
Roughness statistics of Materials A, B and C.

Quantity	Variable	A	B	C
Average height	R_a [μm]	0.9	5.5	19.3
Minimum height	R_v [μm]	4.8	25.7	78.1
Maximum height	R_t [μm]	11.7	46.0	138.5
Average maximum height	R_z [μm]	8.4	36.9	133.1
Root mean square height	R_q [μm]	1.2	7.4	24.0
Kurtosis	R_{ku} [μm]	4.5	4.9	2.9
Skewness	R_{sk} [μm]	−0.5	−1.75	−0.2

Table 2
Relative roughness Reynolds numbers.

Material	k_s	Re_* (0.72 m/s)	Re_* (0.98 m/s)	Re_* (1.15 m/s)
A	6.6	1.1	1.5	1.7
B	36.4	6.3	8.2	9.2
C	125.3	21.8	28.2	31.6

Table 3
Roughness statistics.

Author	Formula	Mat A	Mat B	Mat C
Speidel (1962)	$Rz/5$	1.68	7.38	26.61
Forster (1967)	$Rz/2.56$	3.27	14.42	51.98
Forster (1967)	$2Ra$	1.84	11.08	38.64
Forster (1967)	$7Ra$	6.44	38.78	135.24
Koch and Smith (1976)	$6Ra$	5.52	33.24	115.92
Bammert and Sandstede (1976)	$2.2Ra^{0.88}$	2.04	9.92	29.79
Schaffler (1980)	$8.9Ra$	8.19	49.31	171.95
Barlow and Kim (1997)	$16Ra$	14.72	88.64	309.12
Hoffs et al. (1996)	Rz	8.38	36.92	133.06
Guo et al. (1998)	Rz	8.38	36.92	133.06
Bogard et al. (1998)	$4Ra$	3.68	22.16	77.28
Boyle et al. (2001)	$2.1Rq$	2.54	15.46	50.34
Boyle and Senyitko (2003)	$4.8Rq$	5.81	35.33	115.06
Bunker (2003)	$10Ra$	9.20	55.40	193.20
Shabbir and Turner (2004)	$8.9Ra$	8.19	49.31	171.95
Zhang and Ligrani (2004)	$1.9Rz$	15.92	70.15	252.81
Hummel et al. (2005)	$5.2Ra$	4.78	28.81	100.46
Average		6.6	36.4	125.3

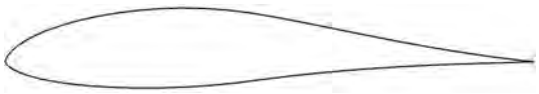

Fig. 5. Shape of the Eppler 715 blade.

and the chord Reynolds number varied from $Re_c = 1.15 * 10^5$ to $Re_c = 2.7 * 10^5$ when the turbine is rotating at $\lambda = 2.0$. The Froude number, based on the water depth and the approach velocity varied between $Fr = 0.35$ and $Fr = 0.52$, confirming that the turbine was subjected to subcritical flows. The influence of blade roughness was examined for different turbine solidities, $\sigma = nc/(\pi D)$, for a three-bladed rotor (by using blades of different chord lengths) and for rotors having different numbers of blades, i.e. rotors with $n = 2$, 3 or 4 10 cm-blades.

3. Results and discussion

The first set of tests used rotors comprising three blades of 8 cm chord length ($\sigma = 0.19$) and made of materials A, B and C, respectively. Their performance was evaluated for the three approach flow velocities. The turbine characteristics curves which are presented in Fig. 6 show that at the lowest flow speed the effect of roughness is fairly small, as all three curves appear to collapse. However, at this low chord Reynolds number the turbine performance is quite poor (C_p<20%). At high flow speed the turbines with blades made of materials A and B behave similarly, reaching peak efficiencies of $C_p = 30\%$,

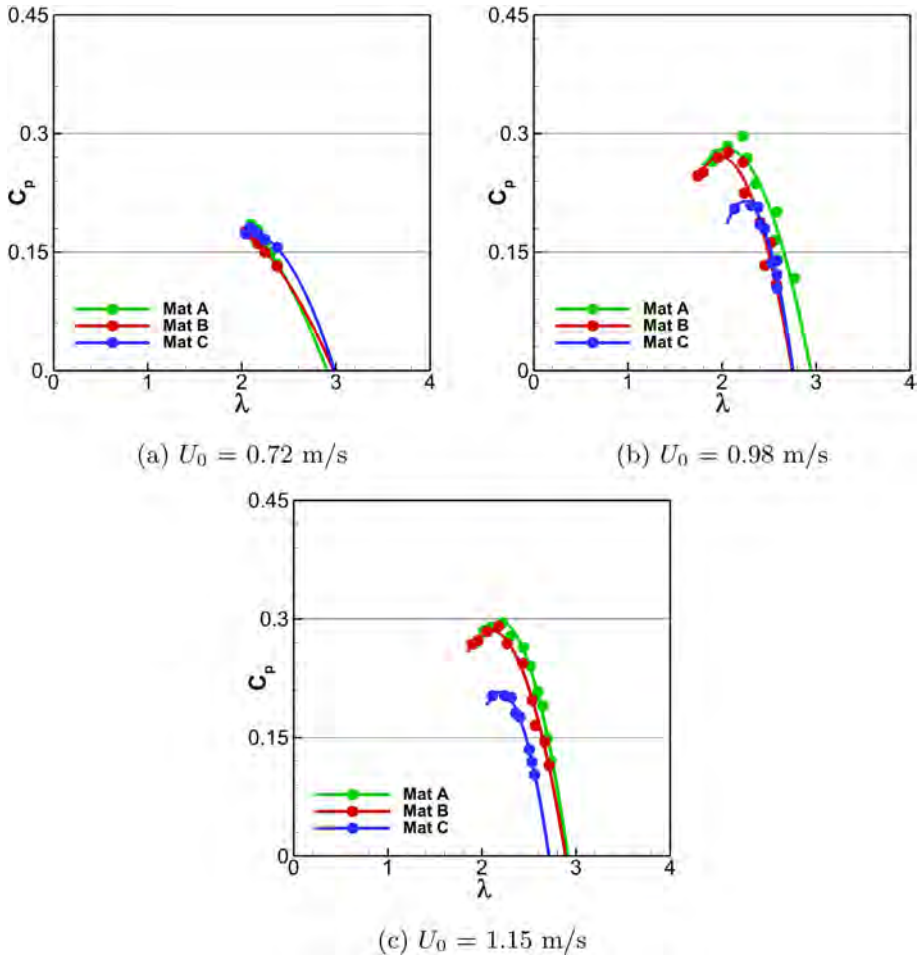

Fig. 6. Turbine performance curves of rotors comprising blades of different materials and for three different flow speeds. Three-bladed rotor, $\sigma = 0.19$.

and both clearly outperform the turbine with the rough blades. The latter only reaches $C_p \approx 20\%$, which is approximately 30% less than turbines featuring smoother blades. It seems clear that the value of Re_* becomes more relevant for high flow speeds or high chord Reynolds numbers, respectively.

Further tests were performed considering rotors that comprise three blades with varying chord length, i.e. 8, 10 and 12 cm, which yielded turbine solidities of σ= 0.19, 0.24 and 0.29, respectively, with the goal of studying the combined effect of blade roughness and turbine solidity. Figs. 7 and 8 present turbine characteristics curves for the low approach and high approach flow speed and for blades made of Materials B and C. As before, the influence of blade roughness is negligibly small for the lowest approach flow velocity. Much more significant is the effect of solidity on turbine performance. The turbine with the smallest blades performs worst with $C_{p,\max} \approx 18\%$, whereas turbines with larger blades, hence higher solidity, achieve $C_{p,\max} \approx 24$–26%. The rotor with c = 10 cm blades performs best for this low flow speed.

As before, blade roughness affects turbine performance negatively at higher chord Reynolds number, as can be seen by comparing the $C_{p,\max}$ values of the two rotors in Fig. 8. The rotor with the highest solidity (c = 12 cm) performs best for $U_0 = 1.15$ m/s, and the performance gain due to using smoother blades is approximately 10%. The low solidity rotor spins faster (i.e. it operates at higher λ) and thus the difference in performance between smooth bladed rotors and rough bladed rotors is more substantial; low-solidity rotors with smooth blades perform approx. 30% better than low-solidity rotors with rough blades.

The results of this study demonstrate that turbines with high rotor solidity outperform low-solidity rotors, which contradicts the design of vertical axis wind turbines where low-solidity turbine rotors have prevailed. Migliore et al. [39] demonstrate that flow curvature effects are detrimental to the performance of wind turbines when rotor solidity is high. On the other hand, [40] note that such effects become less important on curved airfoils and this might explain the fact that water turbines with cambered blades perform better than turbines with symmetrical blades. In fact, Migliore et al. [39] hypothesised that cambered airfoils would experience increased power extraction on the upstream side of the turbine and the diminished efficiency on the downstream side would be more than offset by upstream improvements. The results presented here

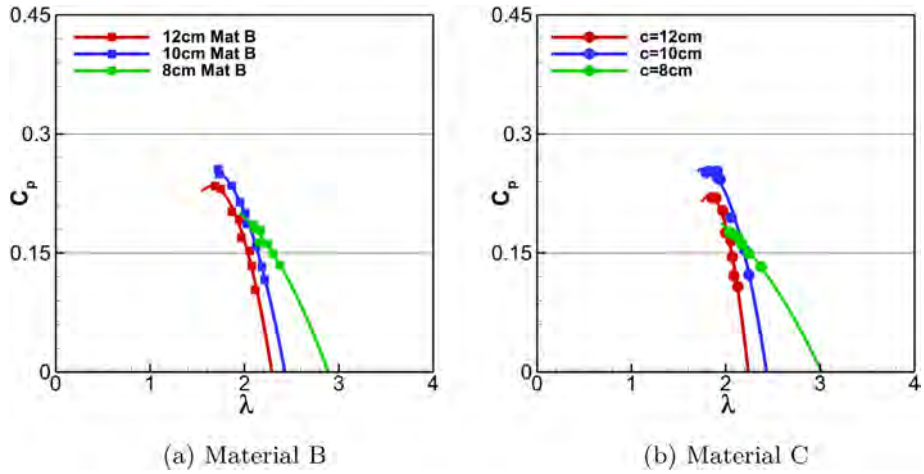

Fig. 7. Turbine performance curves of rotors comprising blades of different materials and different chord length at U_0 = 0.72 m/s. Three-bladed rotor.

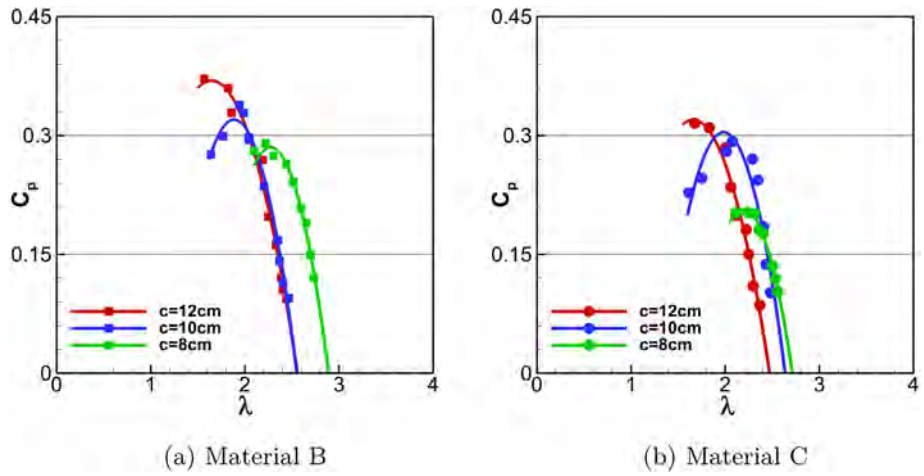

Fig. 8. Turbine performance curves of rotors comprising blades of different materials and different chord lengths at U_0 = 1.15 m/s. Three-bladed rotor.

confirm this hypothesis, in particular for turbines with high solidity, for which flow blockage is large and hence for which power extraction is asymmetric.

Turbine rotors with two, three and four blade configurations (c = 10 cm and $\sigma = 0.16$, $\sigma = 0.24$, $\sigma = 0.32$), were tested with the aim of establishing the additional influence of number of blades on turbine performance. These three different set-ups each have their own advantages and drawbacks. For example, a turbine with two blades is not self-starting and requires a starting torque to begin its rotation. A four-bladed turbine is most likely to be self-starting and gives a steadier torque output over each revolution, but as shown in Fig. 9, four-bladed turbines perform worse than three-bladed turbines, which perform worse than two-bladed turbines. As before, the turbines with smoother blades (Material B) perform better than the ones featuring rougher blades (Material C), most notably at higher speeds, and there the gain in performance is approximately 27% for two-bladed rotors, 33% for three-bladed rotors and 36% for the four-bladed rotor, i.e. the more blades the more influential is blade roughness.

The observations and findings made with the help of Figs. 6–9 suggest that the increase in friction drag due to blade surface roughness cannot be compensated by a possible delay or reduction in flow separation during dynamic stall. The results further indicate that turbine parameters such as rotor solidity or number-of-blades have a similarly profound effect on turbine performance than blade roughness and there also appears to be a "combined rotor parameter effect". In other words, not only is the value of an individual rotor parameter important, it is also important to chose it in knowledge of other rotor parameters. For instance, the two-bladed rotor performs best and it has a rotor solidity of $\sigma = 0.16$ (Fig. 9). In contrast to that the low-solidity three-bladed rotor ($\sigma = 0.19$) performs worst and the three-bladed high-solidity rotor ($\sigma = 0.29$) performs best suggesting that the hydrodynamics (e.g. viscous and wake effects, flow blockage) and fluid–structure interaction play a role too.

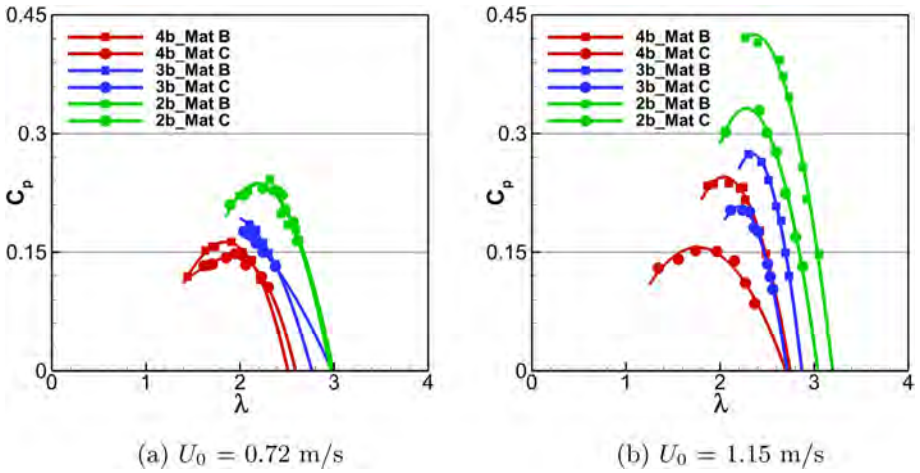

Fig. 9. Turbine performance curves of two-, three- and four-bladed rotors comprising blades of different materials at two flow speeds. c = 10 cm.

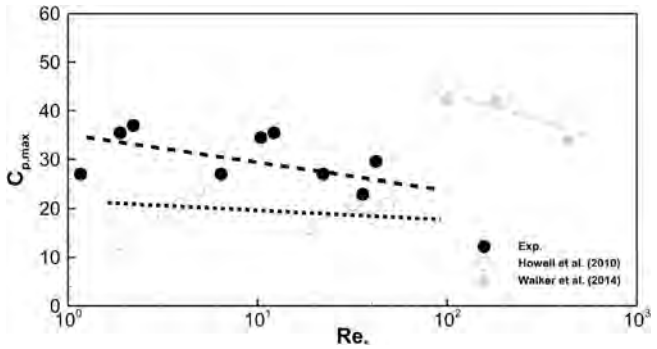

Fig. 10. Maximum coefficient of power as a function of roughness Reynolds number for various studies. Note the roughness Reynolds number for the experiments of [10,11] were estimated in the same way as in this study.

A clear picture of the effects of blade roughness on turbine performance is given with Fig. 10, plotting maximum turbine efficiency, $C_{p,max}$, as a function of roughness Reynolds number, Re_*. Data from the current study is supplemented with the results from [10,11]. At very low roughness Reynolds numbers rotors may benefit from roughening its blades, but the general trend suggests that the rougher the blade the worse the performance of the turbine. The wide spread seen in the current experimental data highlights the importance of other rotor parameters.

4. Conclusions

A series of experimental tests were carried out in the hydraulics laboratory at Cardiff University with the goal of assessing the influence of blade surface roughness on the performance of vertical axis water turbines. Several conclusions can be drawn from the results:

1) It has been shown that blade roughness affects negatively turbine performance and, the rougher the blade, the poorer the performance of the turbine. This is irrespective of other important turbine parameters such as turbine solidity or number of blades.
2) The negative effect of blade roughness is much more significant at high blade Reynolds numbers. At low chord Reynolds number rough-bladed turbines perform as well as smooth-bladed turbines, however at these low chord Reynolds numbers, turbine performance is quite poor anyways.
3) The influence of rotor solidity on the performance of water turbines is high, and this is consistent with existing knowledge. Low-solidity rotors reach higher rotational speeds when compared with their higher solidity counterparts. But high-solidity rotors provide higher torque to the turbine system. In the tests reported herein and at relevant chord Reynolds number, the turbine with the highest solidity rotor performed best.
4) The number of blades per rotor plays a big role in turbine performance too. The two-bladed (low-solidity) rotor performed best, which appears to contradict item 3) suggesting that VATT turbine parameters should not be looked at

in isolation. Generally, the fewer blades the faster the turbine spins, and the more significant the additional effect of blade roughness. In the laboratory tests reported here, the two-bladed rotors did not self-start and their torque output per revolution was much more uneven than for example the four-bladed rotors.

5) The hypothesis that turbines with rough blades could benefit from a delay/reduction of dynamic stall could not be confirmed. Based on the findings presented herein, it should be discarded.

Acknowledgments

The first author is in part sponsored by Repetitive Energy Company (www.repetitiveenergy.com), which is gratefully acknowledged.

References

[1] M.J. Khan, G. Bhuyan, M.T. Iqbal, J.E. Quaicoe, Hydrokinetic energy conversion systems and assessment of horizontal and vertical axis turbines for river and tidal applications: a technology status review, Appl. Energy 86 (10) (2009) 1823–1835.
[2] A.S. Bahaj, A.F. Molland, J.R. Chaplin, W.M.J. Batten, Power and thrust measurements of marine current turbines under various hydrodynamic flow conditions in a cavitation tunnel and a towing tank, J. Renewable Energy 32 (2007) 407–426, http://dx.doi.org/10.1016/j.renene.2007.05.043.
[3] Marine Current Turbines, <http://www.marineturbines.com> (accessed March, 2009).
[4] H. Eriksson, A. Moroso, A. Fiorentino, The vertical axis Kobold turbine in the Strait of Messina – a case study of a full scale marine current prototype, World maritime technology conference, London, 2006.
[5] S. Khalid, Z. Liang, N. Shah, Harnessing tidal energy using vertical axis tidal turbine, J. Appl. Sci. Eng. Technol. 5 (1) (2012) 239–252, ISSN: 2040-7459.
[6] B.R. Kirke, Tests on ducted and bare helical and straight blade Darrieus hydrokinetic turbines, J. Renewable Energy 36 (2011) 3013–3022, http://dx.doi.org/10.1016/j.renene.2011.03.036.
[7] P. Bachant, M. Wosnik, Performance measurements of cylindrical- and spherical-helical cross-flow marine hydrokinetic turbines, with estimates of energy efficiency, J. Renewable Energy 74 (2015) 318–325.
[8] S. Kiho, M. Shiono, K. Suzuki, The power generation from tidal currents by darrieus turbine, J. Renewable Energy 9 (1–4) (1996) 1242–1245.
[9] M.J. Khan, M. Iqbal, J.E.Quaicoe, A technology review and simulation based performance analysis of river current turbine systems, Canadian Conference Electrical and Computer Engineering. Ottawa, Canada (May 2006) 2288–2293. doi:110.1109/CCECE.2006.277821.
[10] R. Howell, N. Qin, J. Edwards, N. Durrani, Wind tunnel and numerical study of a small vertical axis wind turbine, J. Renewable Energy 35 (2) (2010) 412–422, http://dx.doi.org/10.1016/j.renene.2009.07.025.
[11] J.M. Walker, K. Flack, E.E. Lust, M.P. Schultz, L. Luznik, Experimental and numerical studies of blade roughness and fouling on marine current turbine performance, J. Renewable Energy 66 (2014) 257–267, http://dx.doi.org/10.1016/j.renene.2013.12.012.
[12] Y.M. Dai, W. Lam, Numerical study of straight-bladed Darrieus-type tidal turbine, Proc. Inst. Civil Eng. Energy 162 (2) (2009) 67–76.
[13] P. Ouro, T. Stoesser, R. McSherry, Large-eddy simulation of a vertical axis tidal turbine using an immersed boundary method, in: CFD for Wind and Tidal Offshore Turbines, Springer, 2015, pp. 49–58, Chapter 5.
[14] C. Li, S. Zhua, Y.L. Xu, Y. Xiao, 2.5D large eddy simulation of vertical axis wind turbine in consideration of high angle of attack flow, J. Renewable Energy 51 (2013) 317–330, http://dx.doi.org/10.1016/j.renene.2012.09.011.
[15] J. McNaughton, F. Billard, A. Revell, Turbulence modelling of low Reynolds number flow effects around a vertical axis turbine at a range of tip-speed ratios, J. Fluids Struct. 47 (2014) 124–138.
[16] T. Maitre, E. Amet, C. Pellone, Y. Lee, S. Kim, Modeling of the flow in a Darrieus water turbine: wall grid refinement analysis and comparison with experiments, J. Renewable Energy 57 (2013) 497–512, http://dx.doi.org/10.1016/j.renene.2012.09.030.
[17] I. Hwang, S. Min, I. Jeong, Y. Lee, S. Kim, Efficiency improvement of a new vertical axis wind turbine by individual active control of blade motion, Proc SPIE Smart Struct. Integr. Syst. 6172 (2006), http://dx.doi.org/10.1117/12.658935, 8 pages.
[18] I. Paraschivoiu, O. Trifu, F. Saeed, H-darrieus wind turbine with blade pitch control, Int. J. Rotating Mach. 2009 (2009) 1–7, http://dx.doi.org/10.1155/2009/505343.
[19] N. Batista, R. Melicio, J. Matias, J. Catalao, New blade profile for darrieus wind turbines capable to self-start, Renewable Power Generation CRPG IET Conference, 2011, 1–5. doi:http://dx.doi.org/10.1049/cp.2011.0219.
[20] A.J. Fiedler, S. Tullis, Blade offset and pitch effects on a high solidity vertical axis wind turbine, Wind Eng. 33 (3) (2009) 237–246, http://dx.doi.org/10.1260/030952409789140955.
[21] S.-C. Roh, S.-H. Kang, Effects of a blade profile, the reynolds number, and the solidity on the performance of a straight bladed vertical axis wind turbine, J. Mech. Sci. Technol. 27 (11) (2013) 3299–3307, http://dx.doi.org/10.1007/s12206-013-0852-x.
[22] M. Islam, D. Ting, A. Fartaj, Aerodynamic models for darrieus-type straight-bladed vertical axis wind turbines, Renew. Sustain. Energy Rev. 12 (4) (2008) 1087–1109.
[23] Y. Takamatsu, A. Furukawa, K. Okuma, K. Takenouchi, Experimental Studies on a Preferable Blade Profile for High Efficiency and the Blade Characteristics of Darrieus-Type Cross-Flow Water Turbines, JSME Int. J. Ser. 2, Fluids Eng. Heat Transfer Power Combustion Thermophys. Properties 34–II (2) (1991) 149–156, ISSN: 09148817.
[24] B. Yang, X.W. Shu, Hydrofoil optimization and experimental validation in helical vertical axis turbine for power generation from marine current, J. Ocean Eng. 42 (2012) 35–46, http://dx.doi.org/10.1016/j.oceaneng.2012.01.004.
[25] L. Priegue, T. Stoesser, S. Runge, Effect of blade parameters on the performance of a cross-flow turbine, E-proceedings of the 36th IAHR World Congress, The Hague, The Netherlands (June–July 2015).
[26] M. Shiono, K. Suzuki, S. Kiho, An experimental study of the characteristics of a Darrieus turbine for tidal power generation, Electr. Eng. Jpn. 132 (3) (2000) 38–47.
[27] A. Gorlov, Unidirectional helical reaction turbine, U.S. Patent No 5,451,137, U.S. Patent and Trademark Office, 1994.
[28] M. Islam, D. Ting, A. Fartaj, Desirable airfoil features for smaller-capacity straight-bladed VAWT, Wind Eng. 31 (3) (2007) 165–196, http://dx.doi.org/10.1260/030952407781998800.
[29] C. Soraghan, Influence of lift to drag ratio on optimal aerodynamic performance of straight blade vertical axis wind turbines. Europe's Premier Wind Energy Event. Vienna, Austria (February 2013).
[30] K. Standish, P. Rimmington, J. Laursen, H. Paulsen, D. Nielsen, Computational predictions of airfoil roughness sensitivity, in: 48th AIAA Aerospace Sciences Meeting Including the New Horizons Forum and Aerospace Exposition. Orlando, USA, 2010. doi:http://dx.doi.org/10.2514/6.2010-460.
[31] F. Hummel, M. Loetzerich, P. Cardamone, L. Fottner, Surface roughness effects on turbine blade aerodynamics, J. Turbomach. 127 (3) (2005) 453–461, http://dx.doi.org/10.1115/1.1860377.
[32] E. Achenbach, Influence of surface roughness on the cross-flow around a circular cylinder, J. Fluid Mech. 46 (2) (1971) 321–335.
[33] P. Lissaman, Low-Reynolds-number airfoils, Ann. Rev. Fluid Mech. 15 (1) (1983) 223–239.

[34] E. Amet, T. Maitre, C. Pellone, J.L. Achard, 2D numerical simulations of blade-vortex interaction in a darrieus turbine, J. Fluids Eng. 131 (11) (2009), http://dx.doi.org/10.1115/1.4000258 (15 pages).
[35] N. Fujisawa, S. Shibuya, Observations of dynamic stall on Darrieus wind turbine blades, J. Wind Eng. Ind. Aerodyn. 89 (2) (2001) 201–214, http://dx.doi.org/10.1016/S0167-6105(00)00062-3.
[36] Futek advance sensor technology, inc, http://www.futek.com.
[37] J. Nikuradse, Gesetzmaessigkeiten der turbulenten stroemung in glatten rohren, Forschung auf dem Gebiete des Ingenieurwesens 4 (1) (1933), http://dx.doi.org/10.1007/bf02716946, 44 pages.
[38] J.P. Bons, A review of surface roughness effects in gas turbines, J. Turbomach. 132 (2) (2010), http://dx.doi.org/10.1115/1.3066315, 16 pages.
[39] P.G. Migliore, W.P. Wolfe, J.B. Fanucci, Flow curvature effects on darrieus turbine blade aerodynamics, J. Energy 4 (2) (1980) 49–55, http://dx.doi.org/10.2514/3.62459.
[40] D. Coiro, F. Nicolosi, A. De Marco, S. Melone, F. Montella, Flow curvature effects on dynamic behaviour of a novel vertical axis tidal current turbine: Numerical and experimental analysis, in: Proceedings of the 24th International Conference on Offshore Mechanics and Arctic Engineering, Halkidiki, Greece (June 2005).